ISSN: 2277-9655
(I2OR), Publication Impact Factor: 3.785

IJESRT

INTERNATIONAL JOURNAL OF ENGINEERING SCIENCES & RESEARCH TECHNOLOGY

LOW COMPLEXITY ALGORITHM FOR EXTRACTION OF ECG FIDUCIAL POINTS

Mrs. (Patky) Deshpande Punam Subhashrao*, Prof.Halahlli S. R.

ABSTRACT

An automated algorithm for detection of fiducial points from the electrocardiogram (ECG) and identification of its various morphologies is proposed in this work. The application area we consider is that of remote cardiovascular monitoring, where continuous sensing and processing takes place in computationally constrained devices, thus the complexity of the processing algorithms should remain at a minimum level. Under this context, a discrete wavelet transform (DWT) with the Haar function as mother wavelet, is used as principal analysis method in this paper. From the modulus-maxima analysis on the DWT coefficients, an approximation of the ECG fiducial points is extracted. These initial findings are complimented with a refinement stage, based on the time-domain morphological properties of the ECG, which alleviates the decreased temporal resolution of the DWT. The resulting algorithm is a hybrid scheme of time- and frequency domain signal processing.

Conventionally such ECG signals are acquired by ECG acquisition devices and those devices generate a printout of the lead outputs. A cardiologist analyzes the data for checking the abnormality or normalcy of the signal. But in recent times, automatic ECG processing has been of tremendous focus. The main point of concern is how to develop a system for extracting the features from ECG signal so that these features can be used for Automatic Diseases Diagnosis. In this Article We discuss a technique for extracting features from ECG signal and further analyze for 'QRS', 'P-R'& 'S-T' intervals in appropriate time.

KEYWORDS: Electrocardiogram (ECG), Fidicual point detection, Haar wavelet, Maximum Modulus Approximation (MMA), signal processing,, Time domain Marphology (TDM),.

INTRODUCTION

The analysis of the shape of ECG curves as well as the identification of relevant intervals between different waves is of major importance for the diagnosis of cardiac disorders.

The ECG pattern contains a large amount of information about the functionality of the heart as for example its electrical conduction. Amplitudes of the different waves (P, QRS and T wave) as well as particular intervals in a cardiac cycle can indicate an underlying heart disease. The Feature Extraction stage extracts diagnostic information from the ECG signal. Typical ECG signal is as shown in fig.1.

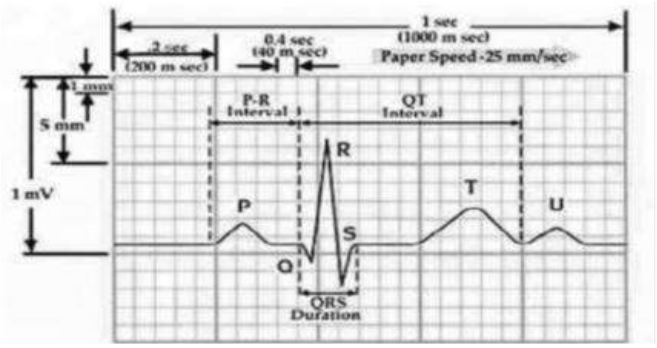

Figure 1.Typical ECG waveform

AGING population and continuous prevalence of cardiovascular diseases (CVD)—the number one cause of death

(30% of the global total of all deaths) according to the World Health Organization (WHO)—leading to long-term conditions, have put current healthcare systems worldwide under serious strain in terms of the quality of care delivery and its associated cost.

Cardiovascular disease monitoring is a big challenge in clinical practice. The cost of CVD care delivery can be reduced by effective disease management through continuous monitoring and information fusion of vital physiological signals in chronic CVD patients. Recently, advances in wireless sensor network (WSN) technology enabled the development of the next-generation remote CVD monitoring and management systems, it is possiable to monitor the patients vital sign data continuously in nomadic environment. The main approach is to use a number of battery-powered wireless sensors to capture the vital signs and transmit all data to a centralized service for further analysis and disease prognosis. Since from a computational perspective the traditional clinical feature extraction algorithms and information fusion techniques are very intensive tasks, these parts are typically executed in main-frame type computational facilities. However, a significant energy expenditure component in such systems is the energy required by the radio front-end for supporting continuous data transmission, which may not allow a long-term sustainable operation. For example, the ECG signal which is the fundamental component of a remote CVDmonitoring system, captured at 1 kHz sampling rate with 16-bit quantization.

Considering a typical Bluetooth V2 transceiver with 40–55 mA current consumption in transmission mode and a battery capacity of 1200 mAh (the typical batteries used for WSN applications) and following the analysis presented in [2], we conclude that the continuous data transmission can be supported only for 24 hours. In addition , the A/D conversion, quantization, and signal preprocessing steps are also carried out at the sensor node. Including these factors, it can be argued that the operation of a continuous transmission based system, may not be realistically sustainable for more than 8–12 h. This falls well below the actual clinical notion of continuous monitoring in the sense of clinical usefulness.

It is important to point out that from a clinical application perspective, the main purpose of the automated ECG analysis in such remote monitoring systems is to produce an “alarm signal” in case an abnormality is detected over a long period of time and by no means perform any detailed diagnosis of the patient’s clinical condition, as this is eventually done through more elaborate diagnostic means (e.g., imaging techniques) in clinical settings.

ALGORITHMIC FORMULATION

In this technique time–domain morphology based ECG feature extraction algorithm, the Fiducial points P, QRS, T are extracted and discrete wavelet transform (DWT) with ‘Haar’ wavelet, is applied on it to detect the presence of points. Detailed DWT coefficients were observed to hypothesize the postulates of detection of all types of morphologies used. Eight patients were randomly selected from the database taken from physionet.

Feature extraction results from ECG signals taken from physionet were tested against manual annotations and used to compare our approach against the state-of-the art ECG delineators. The newly inaugurated Research Resource for Complex Physiologic Signals, which was created under the auspices of the National Center for Research Resources of the National Institutes of Health, is intended to stimulate current research and new investigations in the study of cardiovascular and other complex biomedical signals. The resource has 3 interdependent components. Physio Bank is a large and growing archive of well-characterized digital recordings of physiological signals and related data for use by the biomedical research community. We have taken the input database from the same mentioned site.

The DWT can also be used to construct useful descriptors of a waveform. Since the DWT is a bilateral transform, all of the information in the original waveform must be contained in the sub band signals. These sub band signals, or some aspect of the sub band signals such as their energy over a given time period, could provide a succinct description of some important aspect of the original signal.

WT is advantageous in signal processing for signal analysis but with highest computational cost. Here we used haar wavelet to decompose the signal, as it is simple with less arithmetic operations. It gives approximate coefficient and detailed coefficients. Due to use of haar wavelet power consumption also reduced with lowest computational complexity. Also it reduces noise and isoelectric line wandering in ECG signal.

A. Selecting a wavelet function
B. Haar Wavelet.(Initial estimation of QRS complex)

C. Maximum Modulus Approximation & Time domain marphalology
D. Fiducial point detection.

A.Selecting a wavelet function
Transform can be thought of as a remapping of a signal that provides more information than the original. The Fourier transform fits this definition quite well because the frequency information it provides often leads to new insights about the original signal. However, the inability of the Fourier transform to describe both time and frequency characteristics of the waveform led to the wavelet transform that can be used as yet another way to describe the properties of a waveform that changes over time, but in this case the waveform is divided not into sections of time, but segments of scale.

In wavelet analysis, a variety of different probing functions may be used, but the family always consists of enlarged or compressed versions of the basic function, as well as translations. There are two types of wavelet transforms 1) Continuous wavelet transform (CWT) and 2) Discrete wavelet transform (DWT) The CWT has one serious problem: it is highly redundant. The CWT provides an oversampling of the original waveform: many more coefficients are generated than are actually needed to uniquely specify the signal. This redundancy is usually not a problem in analysis applications such as described above, but will be costly if the application calls for recovery of the original signal. For recovery, all of the coefficients will be required and the computational effort could be excessive. In applications that require bilateral transformations, we would prefer a transform that produces the minimum number of coefficients required to recover accurately the original signal. The discrete wavelet transform (DWT) achieves this parsimony by restricting the variation in translation and scale, usually to powers of 2. When the scale is changed in powers of 2, the discrete wavelet transform is sometimes termed the dyadic wavelet transform which, unfortunately, carries the same abbreviation (DWT).

B.Haar Wavelet
Because of its time-scale analysis nature, it is inherently able to separate noise and artifacts, like iso-electric line wandering with the help of WT, at its different resolution levels as already been shown in [19]. However, the mother wavelet used for this purpose is a computationally demanding quadratic-spline Wavelet and as mentioned previously has an impact on the energy consumption. We have selected the Haar wavelet—the simplest wavelet function to reduce computational complexity and in turn energy consumption. Even the Haar function has its own limitations; we hypothesized that it still may be sufficient for the present purpose. The Haar wavelet function and its corresponding scaling function are depicted in Fig. 2.To ascertain the effectiveness of the Haar DWT in dealing with noise and iso-electric line wandering, few ECG signals sampled at 1 kHz were investigated from the PTB database (PTBDB) [6]. Representative examples of signals that demonstrate iso-electric line wandering and signals that contain a significant amount of noise are illustrated alongside the five decomposition scales of Haar DWT in Fig.3. It is obvious that significant noise components exist in the first two resolution levels.

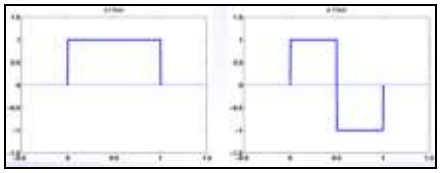

Figure 2: scaling function and Haar wavelet function.

Therefore, applying MMA on these scales could lead to less accurate results. From our observations, we concluded that by employing the MMA on the 23 scale detailed DWT coefficients (cD_l3), an initial estimation of the QRS fiducial points, within the PQRST complex, are possible. Where in the 23 scale, noise components are suppressed to such a degree allowing for a noise-free representation of the ECG signal from the 23 scale onward. Therefore, for identifying the ECG waves, it is sufficient only to consider the 23 (for QRS) and 25 (for P/T waves) resolution scales. This implicitly means substantial reduction in the computational complexity. Nevertheless, operating exclusively on the 23 scale introduces the disadvantage of diminished temporal resolution due to down sampling. This is expected to add inaccuracies in the estimation of the QRS initially assumes the presence of all the constituent ECG waves (P, QRS, and T). Our method is a combination of the MMA applied on the DWT decomposition levels and the time-domain morphological analysis of the ECG signal.

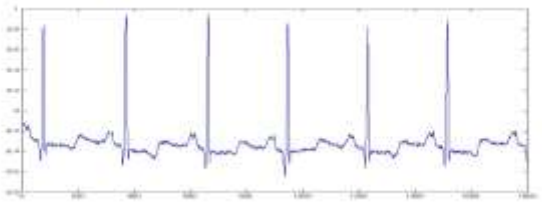

Figure 4: sample ECG signal

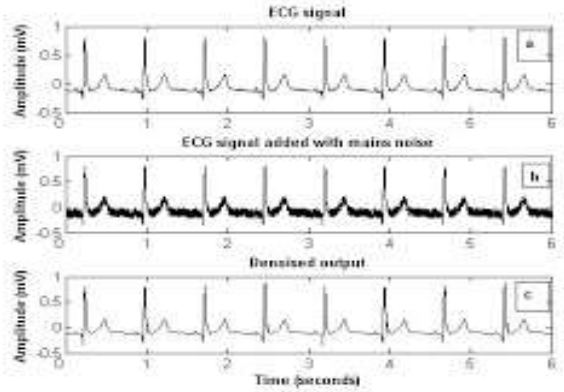

Figure 5: Wandering baseline artifact

The first-level details (d1) show the discontinuity most clearly, because the rupture contains the high-frequency part. The discontinuity is localized very precisely around time = 500. The presence of noise, which is after all a fairly common situation in signal processing, makes identification of discontinuities more complicated. If the first levels of the decomposition can be used to eliminate a large part of the noise, the rupture is sometimes visible at deeper levels in the decomposition. We have zoomed in on the middle part of the signal to show more clearly what happens around time = 500. The details are high only in the middle of the signal and are negligible elsewhere. This suggests the presence of high-frequency information -- a sudden change or discontinuity around time = 500.

The first-level details (d1) show the discontinuity most clearly, because the rupture contains the high-frequency part. The discontinuity is localized very precisely around time = 500. The presence of noise, which is after all a fairly common situation in signal processing, makes identification of discontinuities more complicated. If the first levels of the decomposition can be used to eliminate a large part of the noise, the rupture is sometimes visible at deeper levels in the decomposition. We have zoomed in on the middle part of the signal to show more clearly what happens around time = 500. The details are high only in the middle of the signal and are negligible elsewhere. This suggests the presence of high-frequency information -- a sudden change or discontinuity around time = 500.

To detect a singularity, the selected wavelet must be sufficiently regular, which implies a longer filter impulse response. Regularity can be an important criterion in selecting a wavelet.. With the help of haar wavelet, the discontinuity would not have been detected. The resulting algorithm is referred as the hybrid feature extraction algorithm (HFEA), since we employ both frequency and time domain analysis. To begin with, DWT decomposition takes place on the PQRST-complex. The analysis is performed at five dyadic space scales (21 ,…. 25) using the 23 and 25 scale for the extraction of QRS and P/T waves parameters. With the help of high and low pass filters we can implement multiscale DWT decomposition as a cascade filter bank structure as shown in fig.5. The output of the high-pass filters (H1 (z)) provides the detailed WT coefficients (cD_lx) at the 2x scale, while the approximate WT coefficients (cA_lx) are obtained from the output of the low-pass filters (H0 (z)). From the Haar transfer functions, it can be seen that the output of the high-pass filter is proportional to the local averages of the derivative of the input, which in turn is a filtered version of the original signal. From this, it is established that potential extrema in the original signal x[n] are represented as zero-crossing points in the cD_lx (where x is odd), while instances with maximum slope (deflection points) in the signal are transformed into extrema (minima or maxima) points on the cD_lx.

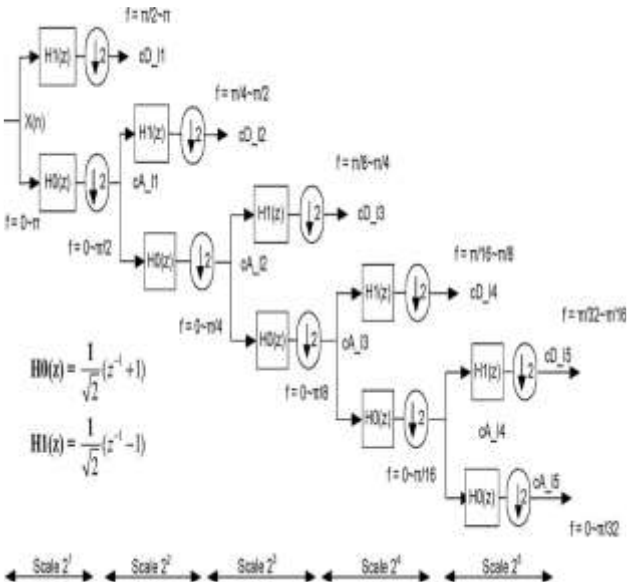

Figure 6: Cascade filter-bank implementation of DWT.

C. Maximum Modulus Approximation & Time domain marphalology

MMA is employed for the approximation of the zero-crossing points after computing wavelet coefficients, the focus turns on the 23 scale detailed coefficients, The boundaries of the constituent ECG waves (P, QRS, and T) are expected based on the MMA principle, due to their morphology (deflection points),to be localized by a modulus-maxima pair (MMP) on the DWT coefficients of the respective scale. Given the positive or negative deflection of the ECG wave, compared to the isoelectric line, for a positive deflection the pair of extrema that indicates the wave's temporal position, can be either a minimum followed by a maximum, or the reverse for a negative deflection. Thus, the MMA method also allows the characterization of every wave as inverted or not, which is exploited in our algorithm. Through MMA, we initially obtain the temporal position of the deflection which demonstrates higher separation from the isoelectric line. This is accomplished by calculating the temporal positions (t1, t2) of the global extrema pair in the cD_l3 coefficients. This deflection may correspond to either the R_peak (for a positive deflection) or to Q or S_peak (in case of a negative deflection). After that, MMA is applied in the vicinity of the global extrema pair, in order to obtain a first approximation of the temporal position of the QRS boundaries. The initial estimation of the QRS onset (QRSon) is obtained as the preceding extrema (min or max) from the local MMP in a search window defined as [t1−4, t1]. Similarly, the offset of the QRS, (QRSon) is estimated from the succeeding extrema of the MMP found in [t2, t2+4].

As pointed out earlier, the temporal resolution on the 23 scale is diminished (by a factor of 8) compared to the original timescale. This coupled with fact that we operate on a single resolution scale, may inherently lead to less accurate localization of the main deflection (Either R_peak or Q, S_peak) and of the QRS boundaries, an example where the MMA produces less accurate results. For mitigating that effect we employ a TDM-based refinement. The TDM refinement process amends the initial MMA approximation, leading to a more accurate estimation of the QRS fiducial points. The R_peak time instance is amended first. From the MMA on the cD_l3, we obtain the temporal boundaries (t1, t2) within which lies the deflection that exhibits higher separation from the isoelectric line. If this deflection is characterized as positive, it is interpreted as an R-wave and thus by projecting (t1, t2) into the original timescale of x[n], the amended R_peak time point is calculated as the maximum of the PQRST-complex (max(x[n])) within this time window ($n \in [t1 \times 23, t2 \times 23]$). If the deflection detected in the MMA is characterized as negative (t1 is a maximum and t2 is a minimum), then it corresponds to either the Q or the S_peak. Since, the R_peak is always a positive deflection; it will be always localized by an MMP with the first point being a minimum and the second a maximum in the cD_l3.

D.Fiducial point detection

After the TDM refinement process QRS boundaries are finalized, At the cD_l3 the same modulus-maxima analysis was applied at the CD_13 is applied at the 25 resolution scale detailed coefficients CD_15 only at the portion that precedes and succeeds the detected QRS complex in order to P and T-wave feature extraction in order to identify the

P and T wave boundaries and the corresponding peaks. P and T waves are known to identify either convexity or concavity against the isoelectric line and the MMP that localizes the wave also allows us to characterize it as convex or concave in a similar way that we characterize a deflection as positive or negative. The complete HFEA algorithm is given in the form of pseudo code in Fig.7. The implementation of the algorithm for validation took place in MATLAB.

RESULTS AND DISCUSSION

We present here an analytical calculation of the number of arithmetic operations required for the HFEA to run to completion to quantify the complexity of the HFEA algorithm. There are three major components in the HFEA:

1. DWT coefficients generation
2. MMA
3. TDM refinement

For analysis, subtractions are considered equivalent to additions, while one comparison operation is considered to have half the complexity of an addition. For extraction of extremas (min/max) within a specific interval Comparisons are used. According to the Haar DWT high- and low-pass filter transfer functions, we consider that for a single cD_lx or cA_lx coefficient, 1 addition, and 1 multiplication is required to derive the number of arithmetic operations required. For the DWT coefficients generation, as an example, in order to calculate the cD_l1 or cA_l1 coefficients individually, N/2 additions and N/2 multiplications are required. Subsequently, the calculation of cD_l2 or cA_l2 requires N/4 additions and N/4 multiplications. In the HFEA, we only utilize the cD_l3, cA_l3 and cD_l5 coefficients, which according to Mallat's algorithm, means that from the other resolution scales only cA_l1, cA_l2 and cA_l4 must be calculated. Since cD_l5 are computed directly from cA_l4 the cA_l5 coefficients do not need to be calculated. In total, the computational complexity of calculating the coefficients that are employed in the HFEA is N/2 + N/4 + 2N/8 + N/16 + N/32 additions and N/2 + N/4 + 2N/8 + N/16 + N/32 multiplications. The MMA step involves the extraction of the max and min values of cD_l3, which is of N/8 length. This process requires (N/8 − 1) comparisons. The additional MMA calculations in the vicinity of the global MMA pair require 2 additions for the expansion of t1, t2 , 4 comparisons in the [t1 − 4, t1] interval and another 4 comparisons in the [t2, t2 + 4] interval ,thus in total 6 additions. At this point the TDM refinement step takes place. The t1, t2 values, obtained from MMA, define an interval of length T in the cD_l3 subspace. For the R_peak extraction, the first possibility where t1 < t2, (positive major deflection) involves the projection of the T interval boundaries to the original timescale with 2 multiplications, where an interval of length 8 T is now defined and for the extraction of the R_peak (8T − 1) comparisons are required to localize the maximum point and designate it as the R_peak .

The second scenario where t2 < t1 (negative major deflection, requires 2 additions for the expansion of t1, t2 values by 15 and 10, respectively, ((15 − 1) + (10 − 1) = 23) comparisons for deriving the ta and tb values, 4 multiplications for projecting the t1, t2, ta, tb into the original timescale and a total of (8 * 15 − 1) + (8*10 − 1) + 1 = 199 comparisons for the localization and comparison of the R_peak1 and R_peak2 values. The final R_peak is mapped back to 23 scale subspace, with 1multiplication, where it is used for the QRS boundaries refinement beginning with setting the adaptive thresholds, for which (N + 2) comparisons, 1 addition and 1 multiplication are required.

The refinement will take place on a sample of M + 23 cA_l3 coefficients. For the backward difference operation (gradient calculation) in that sample, (M + 22) additions are required. The operation of comparing the gradient to the thresholds requires, M + 20 comparisons for identifying both QRSon and QRSoff After projecting the QRS boundaries to the original timescale with 2 multiplications, the final stage of the TDM which pertains to the extraction of the Q and S_peak position which requires, 8(M+ 23)−(1±2) comparisons, where _1, _2 are the differences in samples in the original timescale between the beginning of the 8(M + 23) interval and the detected QRSon and QRSoff and the end of the 8(M + 23) interval respectively. From the above, the TDM stage collectively requires 11M + N + 203-1/2(1±2) comparisons, M + 24 additions and 6 multiplications, for the first if-statement of the TDM and by following the same process 9M + N + 426 − 1/2(1±2) comparisons, M+26 additions and 8 multiplications for the else statement. To sum up the calculation of the TDM stage, we consider that M <N/8,T <M/4 thus T <N/32.Moreover, from our experiments _1, _2 < 30.With these in mind and by expressing comparisons as half additions the total computational complexity of the TDM stage is 1.31N + 95 additions, 6 multiplications, or 1.18N + 208 additions, eight multiplications depending on which if-statement is satisfied.

ISSN: 2277-9655
(I2OR), Publication Impact Factor: 3.785

1.Initialise

Consider a PQRST complex x[n] of length *l*

2. HAAR DWT

Calculate DWT Approximate cA l3 and Detailed Coefficients

cD l3 and Detailed Coefficients.

3. QRS Initial Estimation

Display approximate and detail coefficients.

Get minimum and maximum values from level 3 detail coefficients.

4. Save A3 to temporary variable.

Save D3 to temporary variable.

5.Time-Domain Refinement (TDM)

Refinement for Q position using approximate coefficients

Set 1 to S position equal to minimum value.

Get T position from remaining temporary signal.

6.P,T Wave Estimation MMA

Save to temporary variable.

Set Q position to last A3 equal to minimum value.

Get P position from remaining temporary signal.

REPEAT P Block with n ∈ [QRSoff cD l5 end] for the Twave

7.Plot signal and show PQRST points.

8.Calculate QRS PR ST intervals at level 3.

9.Calculate QRS PR ST intervals in time domain

10.Convert QRS PR ST intervals in appropriate seconds.

Figure 7: .HFEA Algorithm for ECG feature extraction

The final stage of the HFEA for the extraction of the P and T wave fiducial points initially requires the MMA analysis on the cD_l5 coefficients. For the P-wave, the MMA can theoretically run on a maximum of N/64 coefficients and may require up to (N/64 − 1) comparisons to extract the max and min points. Localizing, through MMA, the min and max point of cD_l5 defines an interval of length P which after being projected (with 2 multiplications) in the original timescale has a length of 8P. In this interval the P peak time instance is localized, as the min or max value of the interval and for this (8P − 1) comparisons are used.

As P <N/80 from experiment, the equivalent number of additions for the P-wave analysis is 0.0391N − 1 additions and 2 multiplications. For the T-wave analysis, the same number of operations is considered to be required, thus the total number for this stage is 0.0875N − 2 additions and 4 multiplications. From the above investigation, the total number of operations required for the HFEA algorithm is 2.553N + 102 additions and 1.093N + 10 multiplications, or 2.423N + 214 additions and 1.093N + 12 multiplications based on which if-statement is executed on the R peak extraction. This final number represents an upper bound on the required arithmetic operations.

It is obvious that the upper bound depends on the number of input samples N. By considering the number of multiplications to be approximately the same for both cases, we focus on the number of additions and conclude that for N ≤ 861 the upper bound is 2.423N + 214, while forN >861 the upper bound is 2.553N + 102. In reality, the number of actual arithmetic operations is going to be lower since M _ N/8, T _ N/32 and the MMA on cD_l5 will be executed on a smaller than N/64 number of coefficients.

Now it is compared with WT ECG delineator. This work creates the basis of WT-based ECG delineation the quadratic-spline wavelet is used to avoid decimations. We observe from the transfer function provided, that for computing a single pair of WT coefficients 4 additions and 4 multiplications is required. Since, the number of generated WT coefficients in each level is the same as the number of input samples, for an input of N samples 4N additions and 4N multiplications are required to generate the WT coefficients in one level. 17N additions and 17N multiplications are needed for the DWT coefficients generation for the first five scales of WT coefficients. Approximate coefficients of the 25 are not computed. It is obvious that the amount of required arithmetic operations only for the calculation of the WT coefficients in [16], without any further processing, is considerably higher that the upper bound of the computational complexity of the HFEA. This is indicative of the possibility for significant power reduction, compared to the WT-delineator of [16], of the HFEA when implemented.

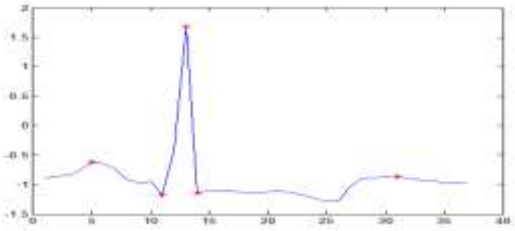

Figure8: accurately detected PQRST peak points

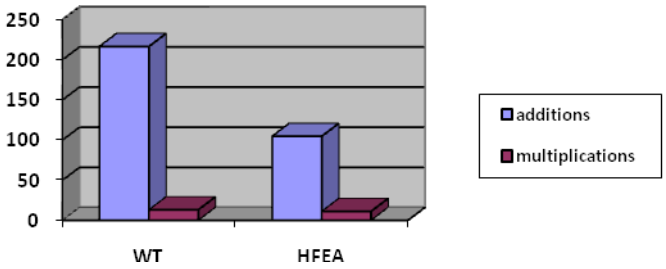

Fig.9: computational complexity in HFEA

CONCLUSION

A novel algorithm (HFEA), based on the combination of WT analysis, MMA and time-domain morphology principles, for extracting the ECG fiducial points is proposed in this paper. The use of DWT with the Haar function as the basis allows for a significant reduction in the computational complexity compared to other WT-based approaches. Fig.8 shows an output indicating Fiducial points of an ECG with red colour with asterisk. In order to assess the performance of the proposed algorithm andquantify its accuracy, ECG signals from various databases from physionet are used. These signals are manually annotated with the help of expert chest therapist. HFEA demonstrated the best performance of the three algorithms and there are no CSE tolerance limits.

For these parameters it is observed that the CSE limit is not satisfied, and the error in terms of the actual ECG samples, except from T_peak. HFEA performance is very close to the state-of-the-art ECG delineators. By taking into account that mobile CVD monitoring systems are predominantly used for assessing the patient's overall condition, rather than making a complete diagnosis, the proposed scheme is comparatively better for the ECG analysis in such systems.

REFERENCES

[1] Rinc´on, J. Recas, N. Khaled, and D. Atienza, "Development and evaluation Of multilead wavelet-based ECG delineation algorithms for embedded wireless sensor nodes," IEEE Trans. Inf. Technol. Biomed., vol. 15, no. 6,pp. 854–863, Nov. 2011.

[2] R. Balani, "Energy consumption analysis for bluetooth,WiFi and cellular networks," Univ. California at Los Angeles, Tech. Rep. TR-UCLA-NESL-200712-01, 2007

[3] A. L. Goldberger *et al.*, "Physiobank, physiotoolkit, and physionet components of a new research resource for complex physiologic signals," *Circulation*, vol. 101, no. 23, Jun. 13, 2000.

[4] R. V. Andre˜ao, B. Dorizzi, and J. Boudy, "ECG signal analysis through Hidden Markov Models," *IEEE Trans. Biomed. Eng.*, vol. 53, no. 8, pp. 1541–1549, Aug. 2006.

[5] Z. Yong, H. Wenxue, X. Yonghong, and C. Jianxin, "ECG beats classification based on ensemble feature composed of independent components and QRS complex width," in *Proc. Int. Conf. Comput. Sci. Softw. Eng.*,Dec. 2008, vol. 1, pp. 868–871.

[6] S. Szil´agyi and L. Szil´agyi, "Wavelet transform and neural-network based adaptive filtering for QRS detection," in *Proc. IEEE Eng. Med. Biol. Soc.*,Jul. 2000, vol. 1, pp. 1267–1270.

[7] S. Szilagyi, Z. Benyo, L. Szilagyi, and L. David, "Adaptive wavelettransform-based ECG waveforms detection," in *Proc. IEEE Eng. Med. Biol. Soc.*, Sep. 2003, vol. 3, pp. 2412–2415.

[8] R. V. A. Andre˜ao and J. Boudy, "Combining wavelet transform and hidden Markov models for ECG segmentation," *EURASIP J. Appl. Signal Process.*, vol. 2007, pp. 95–95, Jan. 2007

[9] G. de Lannoy, B. Frenay,M. Verleysen, and J. Delbeke, "Supervised ECG delineation using the wavelet transform and hidden Markov models," in *Proc. Conf. Int. Federation Med. Biol. Eng.*, 2008, vol. 22, pp. 22–25.

[10] S. Mahmoodabadi, A. Ahmadian, M. Abolhasani, M. Eslami, and J. Bidgoli, "ECG feature extraction based on multiresolution wavelet transform," in *Proc. IEEE Eng. Med. Biol. Soc.*, Jan. 2005, pp. 3902–3905.

[11] K. Ouni, S. Ktata, and N. Ellouze, "Automatic ECG segmentation based on Wavelet Transform Modulus Maxima," in *Proc. IMACS*, Oct. 2006, vol. 1, pp. 140–144.

[12] A. Josko, "Discrete wavelet transform in automatic ECG signal analysis," in *Proc. IEEE Instrum. Meas.Technol.Conf.*,May 2007, pp. 1–3.

[13] Y. Velchev and O. Boumbarov, "Wavelet transform based ECG characteristic points detector," in *Proc. Int. Sci. Conf. Comp. Sci.*, 2008, vol. 1,pp. 22–25.

[14] J. Martinez, R. Almeida, S. Olmos, A. Rocha, and P. Laguna, "A waveletbased ECG delineator: evaluation on standard databases," *IEEE Trans.Biomed. Eng.*, vol. 51, no. 4, pp. 570–581, Apr. 2004.

[15] A. Burns *et al.*, "ShimmerTM—Awireless sensor platform for noninvasive biomedical research," *IEEE Sensors J.*, vol. 10, no. 9, pp. 1527–1534, Sep.2010.

[16] P. Laguna, R. Mark, A. Goldberg, and G. Moody, "A database for evaluation of algorithms for measurement of QT and other waveform intervals in the ECG," in *Proc. Comput. Cardiol.*, Sep. 1997, pp. 673–676.

[17] Laguna, P., Jané, R. and Caminal, P. 1994. Automatic detection of wave boundaries in multilead ECG signals: validation with the CSE database, Comput Biomed Res,Feb, **27(1)**,45-60

[18] Svenja Kutscher ,Högskoleplan 1 721 23 Västerås +46769004298 ,skr12002@student.mdh.se , Algorithms for ECG Feature Extraction: an Overview ,Mälardalen University, School of Innovation, Design, and Technology.

[19] Evangelos B. Mazomenos, Dwaipayan Biswas, Amit Acharyya, Taihai Chen, Koushik Maharatna, *Member*, *IEEE*,James Rosengarten, John Morgan, and Nick Curzen IEEE JOURNAL OF BIOMEDICAL AND HEALTH INFORMATICS, VOL. 17, NO. 2, MARCH 2013, A Low-Complexity ECG Feature Extraction Algorithm for Mobile Healthcare Applications